

Numerical investigation of Catalytic Fast Pyrolysis process in a pilot scale circulating fluidized bed reactor using CFD-DEM-Reaction Kinetics modeling approach



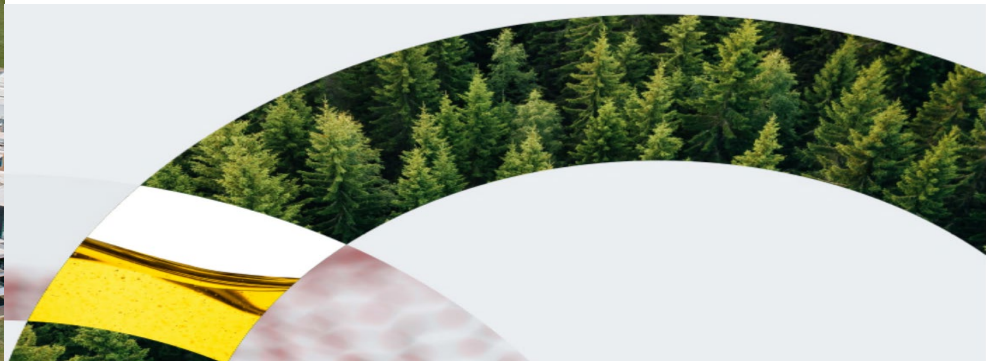
Sheikh Ahmed^{1*}, David Dayton², Thomas Foust¹

¹National Renewable Energy Laboratory (NREL)

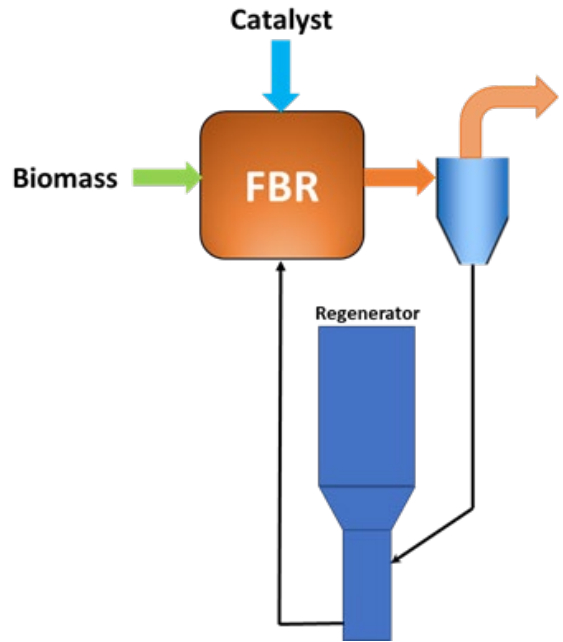
²RTI International



tcbi  **mass**
The International Conference on Thermochemical
Conversion Science:
**Biomass & Municipal Solid Waste to RNG,
Biofuels & Chemicals**



Achieving Net Zero Carbon Goals – the Role for Biomass
April 19–21, 2022
Marriott Brown Palace Hotel and Spa
Denver, Colorado

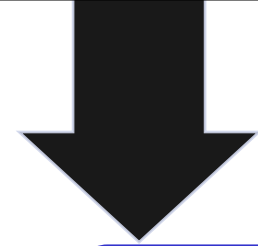


***In-situ* continuously regenerating, circulating fluidized bed pyrolysis and upgrading reactor configuration**

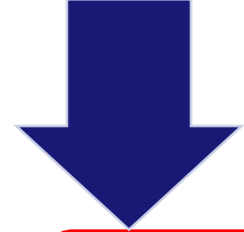
Advantages

- low oxygen-content bio-oil, readily upgraded to transportation fuels
- low capital and operational cost
- greater interactions of particles and phases with respect to contact forces, heat and mass transfer and chemical reactions
- uninterrupted biocrude production with faster reaction rate and advanced heat and mass transfer efficiency

Polymerization of aromatic hydrocarbons



High catalyst coking rate



Rapid catalyst deactivation

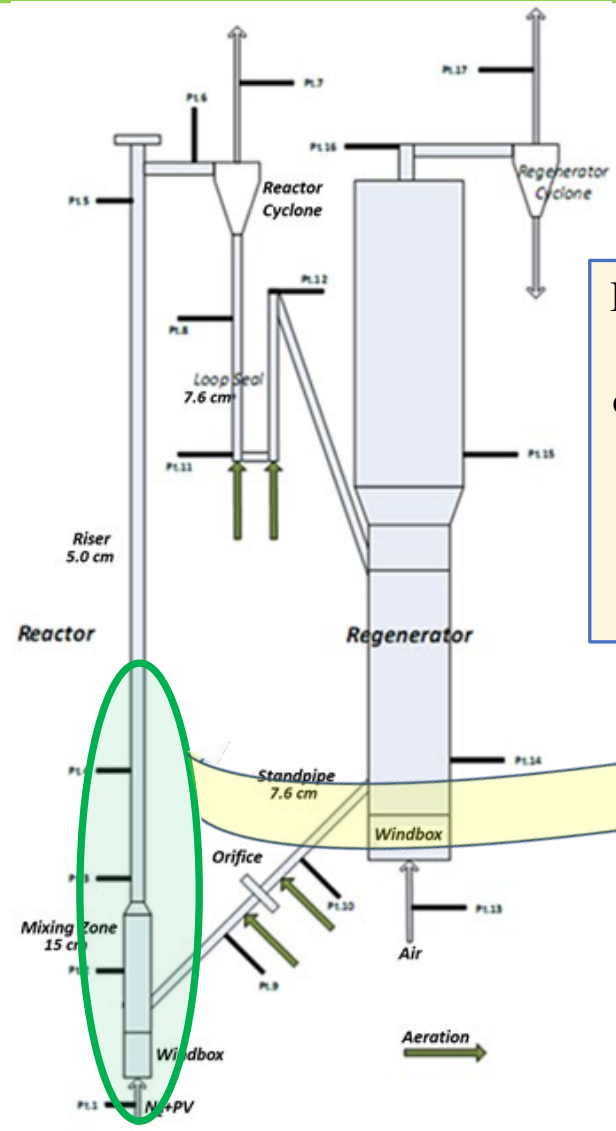
- Process factor optimizations-**
- Vapor residence time in FB
 - Overall reactor configuration



Computational techniques to probe the multiscale gas-solid flow characteristics

- Challenges**
- ❑ *Computational overhead stemmed from multiple length scales*
 - ❑ *Incorporate reaction kinetics with catalyst deactivation*
 - ❑ *Accurately capture S-S, S-G interactions*
 - ❑ *Capture the upgraded product yields*

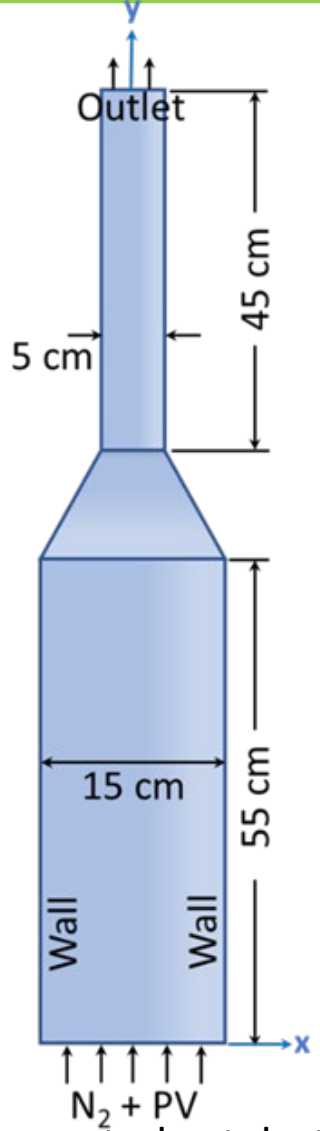
A comprehensive multiphase CFD-DEM model of pyrolysis vapor upgrading in a pilot scale FB reactor system with lumped reaction kinetics



RTI data shows the majority of the catalytic chemistry occurs in the mixing zone and the bottom section of the riser

- Focus of the investigation is to simulate the catalytic upgrading process
- CFD-DEM approach is computationally intensive

Mixing zone + bottom section of the riser



Computational domain

- Upward flow of pyrolysis product gases and vapors
- Catalyst and char particles entrained with the flow

- 300 μm , $\sim 0.68 \text{ M}$ HZSM-5 catalyst particles at 500°C are initially set at the bottom of the mixing zone
- Mass inlet boundary at the inlet specify 500°C $\text{N}_2 + \text{PV}$ and 700°C, $\sim 0.25 \text{ M}$ hot regenerated catalyst particles per second
- $U_f = 3.5 \text{ m/s}$ and $U_g = 0.2 \text{ m/s}$ at the inlet to achieve the closed-loop transport

Partial process flow diagram of RTI 1 TPD circulating CBP unit

Multiphase Flow with Interphase eXchange (MFIx)

Open-source code developed by NETL Multiphase Flow Science group

Euler-Euler model or Two-Fluid-Model (TFM)

Lagrange-Euler model or Discrete Element Model (DEM)

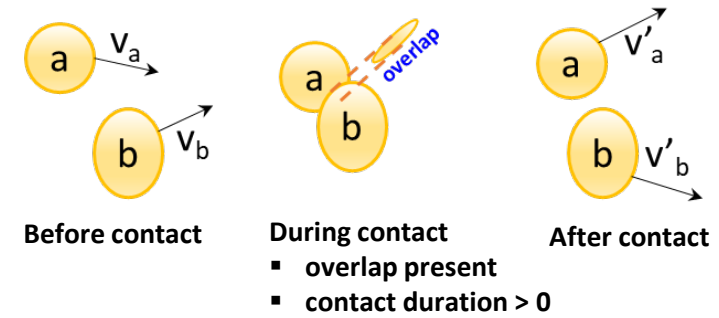
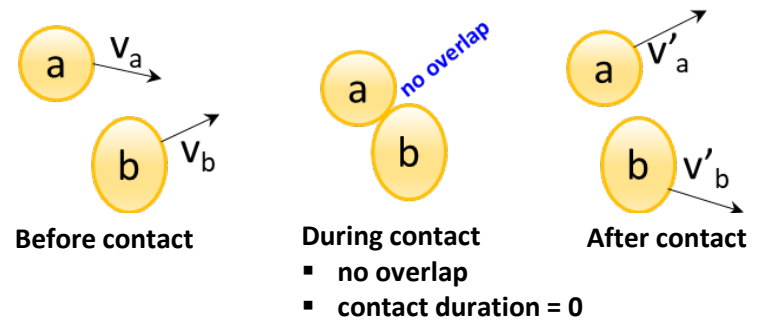
- More physically representative for a dense particulate system
- Advancements in computational resources

P-P and P-W interactions (DEM Model)

Hard Sphere Model

Soft Sphere Model

- Best suited for dense gas-solid flows
- Allows multiple particle collisions with overlaps

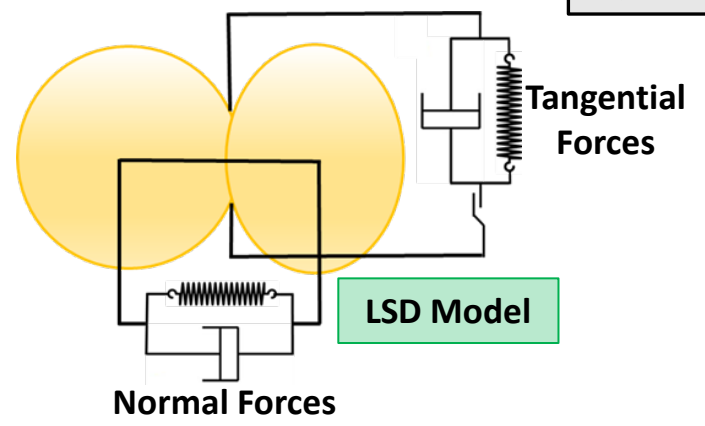


P-P Interaction Models (Elastic, damping and rotational forces during collision)

Nonlinear Hertzian Spring-Dashpot (HSD) model

Linear Spring-Dashpot (LSD) model

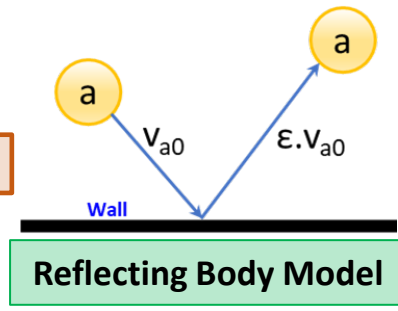
Easy to implement the spring, dashpot and slider element equations in the model



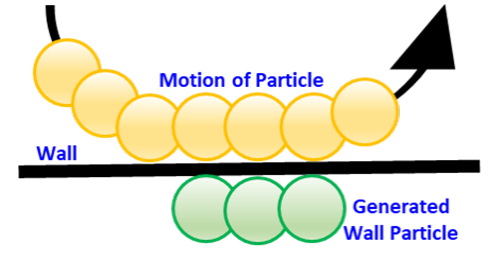
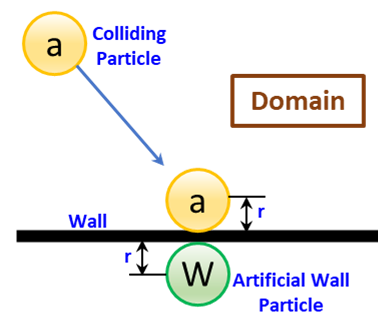
P-W Interaction Models (Neighbor particle replaced by wall with zero velocities)

Reflecting Body model

Wall Particle model



- Less computationally intensive
- More physically representative

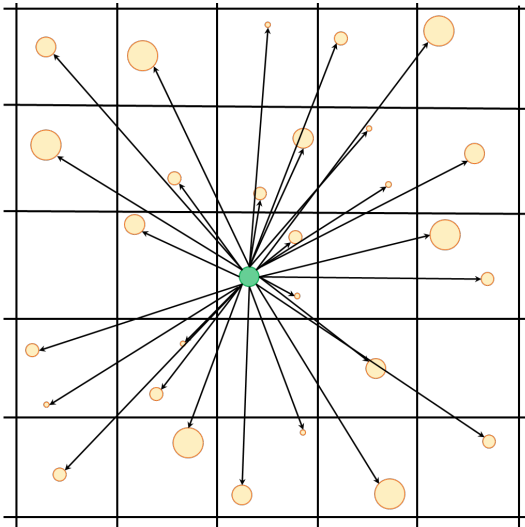




Wall Particle Model

Neighbor list of each particle is required at every time step
One of the most important and time-consuming steps

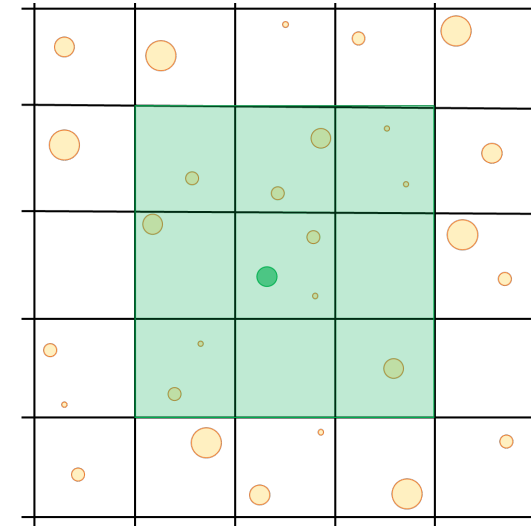
Search algorithms

N² Search (Grid-free search)



-  Particle of interest
-  Neighbor particles

Grid-based Search



➤ Less expensive for large number of particles

Interphase heat transfer methods

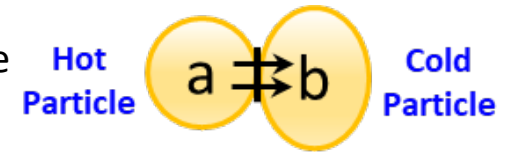
Interphase heat transfer for particle i :

$$q_{gs}^i = \underbrace{q_{pp}^i}_{\text{Contact conduction}} + \underbrace{q_{pfp}^i}_{\text{Particle-fluid-particle conduction}} + \underbrace{q_{pg}^i}_{\text{Gas-particle convection}} + \underbrace{q_{rad}^i}_{\text{Particle-environment radiation}}$$

Negligible P-P, P-W and P-G radiative heat transfer

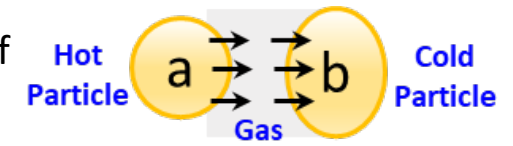
Contact conduction

Energy transfer from a hot to a cold particle through their shared area of contact in the dense particulate system (Batchelor and O'Brien model):



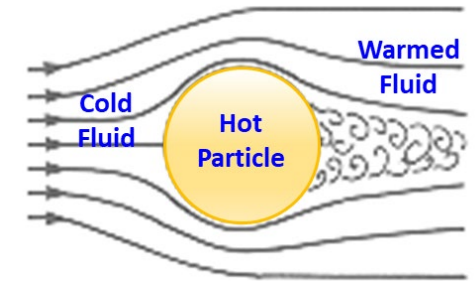
Particle-gas-particle (pgp) conduction

Energy transfer by conducting heat through the stagnant gas between two particles of proximity (modified Rong and Horio correlation):



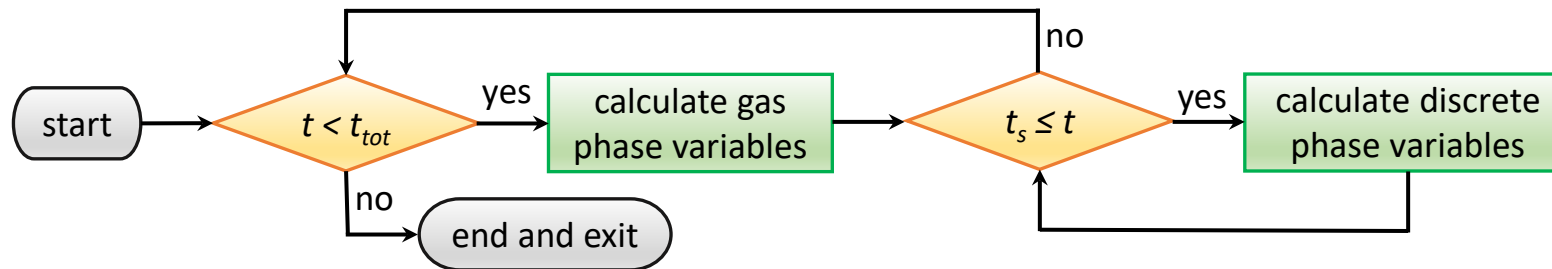
Gas-particle convection

The convective energy transfer between a particle and its surrounding gas (Ranz and Marshall correlation):



Exchange of info between gas and solid particles (Fluid step forward – Particle catch-up process)

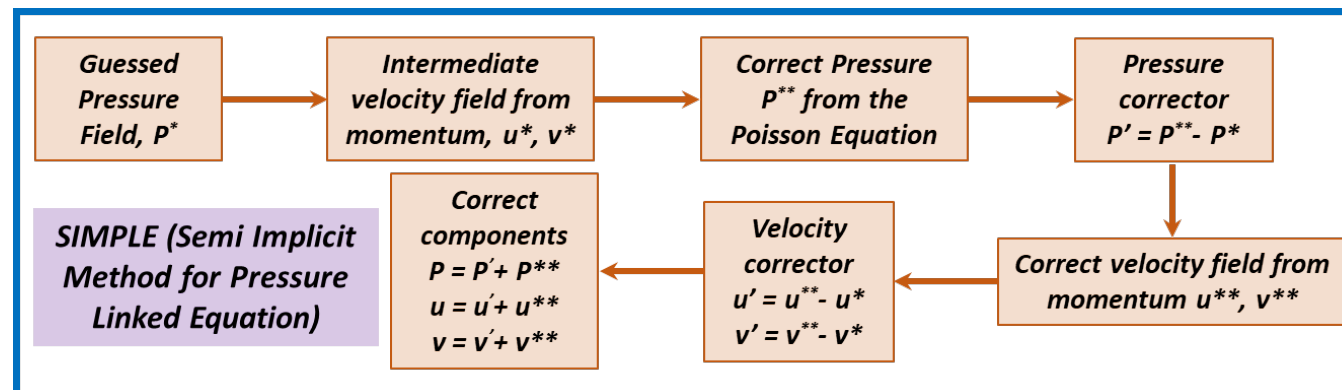
- Gas-solid interactions for circulating FB Reactor is always changing
- Important to computationally connect the vapor phase and solid catalyst particles
- Decide when information is exchanged between gas and solid phases during simulation



t = fluid most recent solution time
 t_{tot} = total specified solution time
 t_s = solid most recent solution time

Gas phase pressure-velocity coupling (SIMPLE algorithm)

- Gas flow field of circulating FB Reactor is sophisticated and challenging to capture
- One of the most computationally intensive parts of the CFD simulation



- Accurate to capture the reactor flow field
- Less expensive with one predictor and one corrector step

Lumped reaction scheme with intrinsic kinetic parameters (NREL)

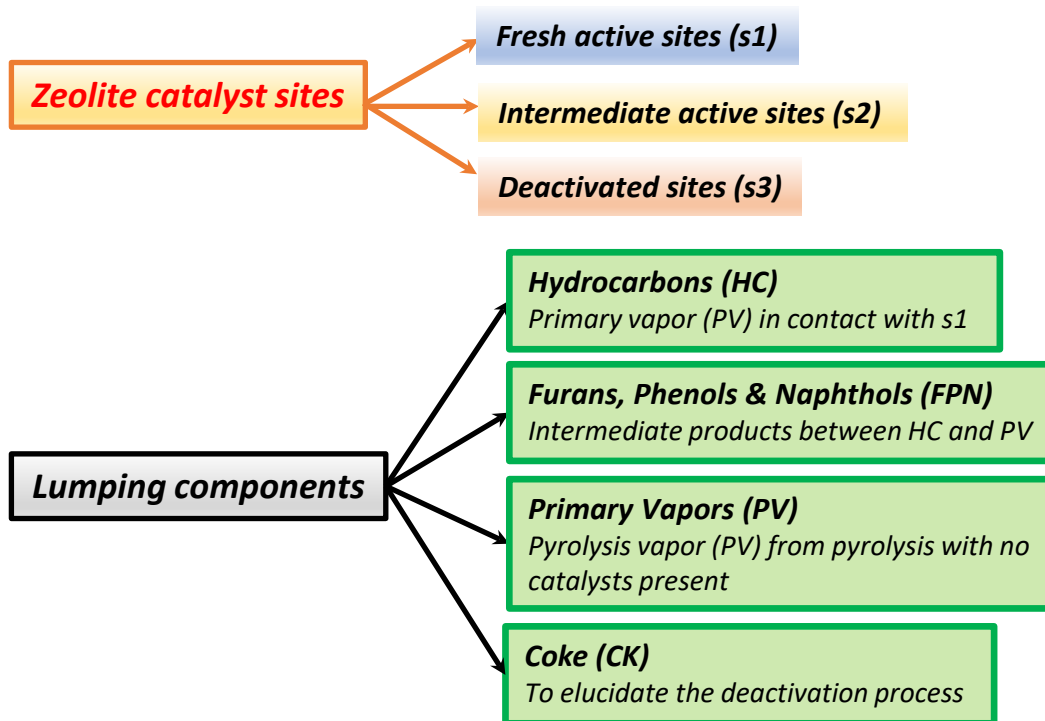
A detailed atomistic micro-kinetic modeling of the CFP process using zeolite kinetics involves broadly diverse species within PV

Literature lumped kinetic models $\left\{ \begin{array}{l} \text{lack of catalyst deactivation reaction} \\ \text{does not account for intraparticle transport} \end{array} \right.$

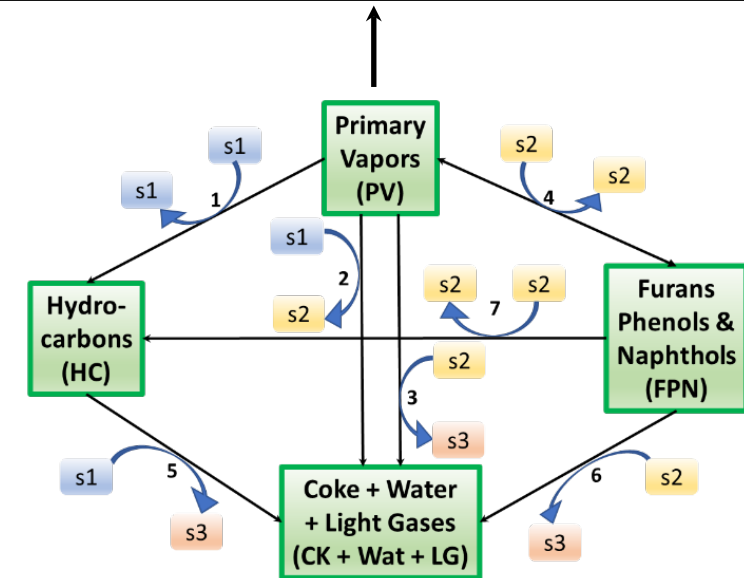
- CFP experiments with loblolly pine over ZSM-5 performed in a spouted bed reactor coupled with MBMS (monitor catalyst deactivation) and GCMS (dynamic product quantification)
- Multi-variate analysis develops a lumped reaction scheme based on the experiments

No.	Reaction	k [m ³ /(mol.s)]
1	PV + S1 → HC + S1	2.5728
2	PV + S1 → [CK + Wat + LG] + S2	0.4561
3	PV + S2 → [CK + Wat + LG] + S3	0.1523
4	PV + S2 → FPN + S2	2.9039
5	HC + S1 → [CK + Wat + LG] + S3	0.5073
6	FPN + S2 → [CK + Wat + LG] + S3	0.0060
7	FPN + S2 → HC + S2	0.0509

Optimization of the rate constants to reproduce experimentally observed HC and FPN trends

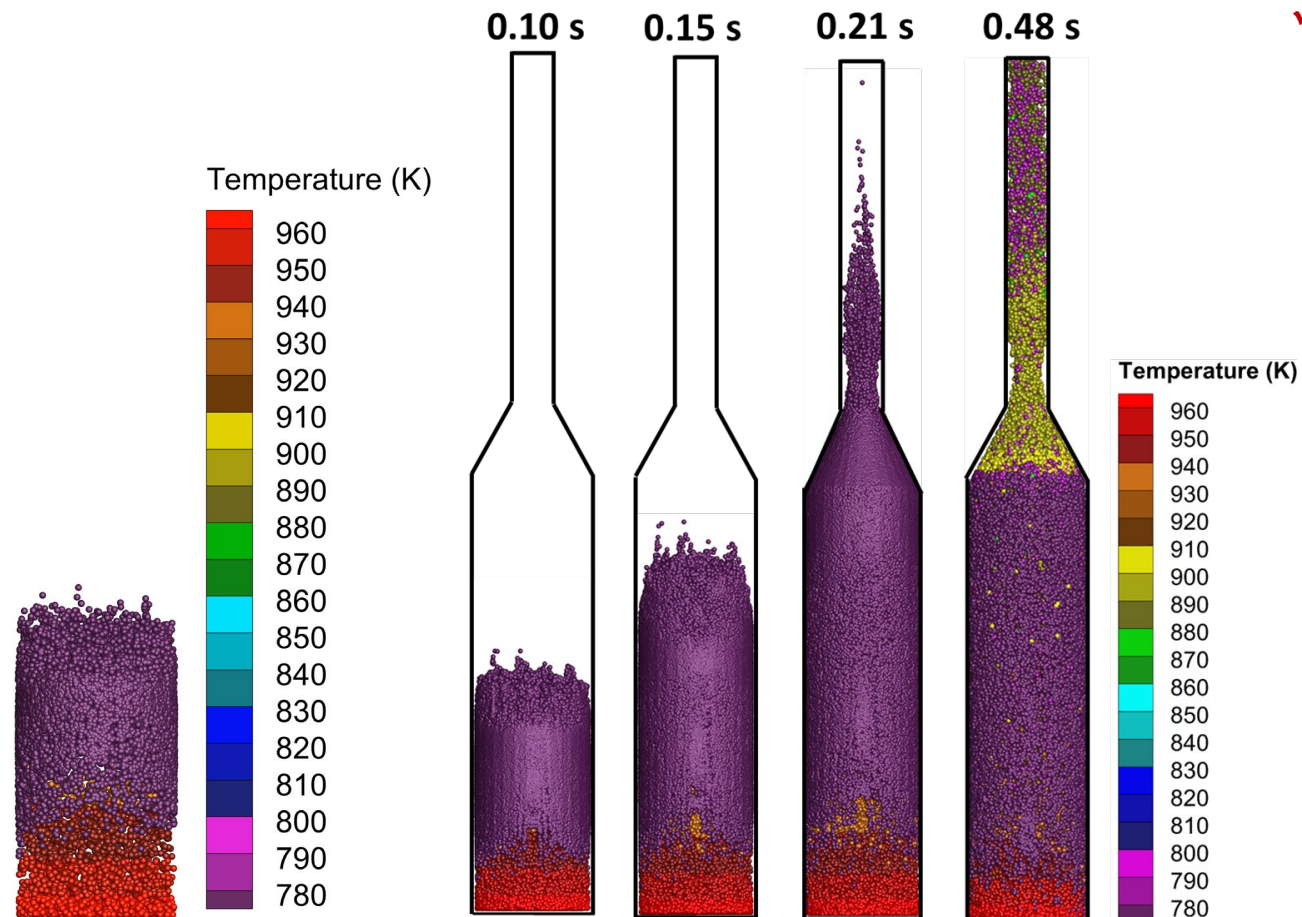


Particle scale FEM framework to capture transport phenomena



Fluidization and hydrodynamic behavior (simulation without chemical reactions)

- 300 μm HZSM-5 catalyst bed at 500°C
- 500°C, N₂+PV and 700°C hot regenerated catalyst particles at the inlet
- $U_f = 3.5 \text{ m/s}$ and $U_g = 0.2 \text{ m/s}$ at the inlet

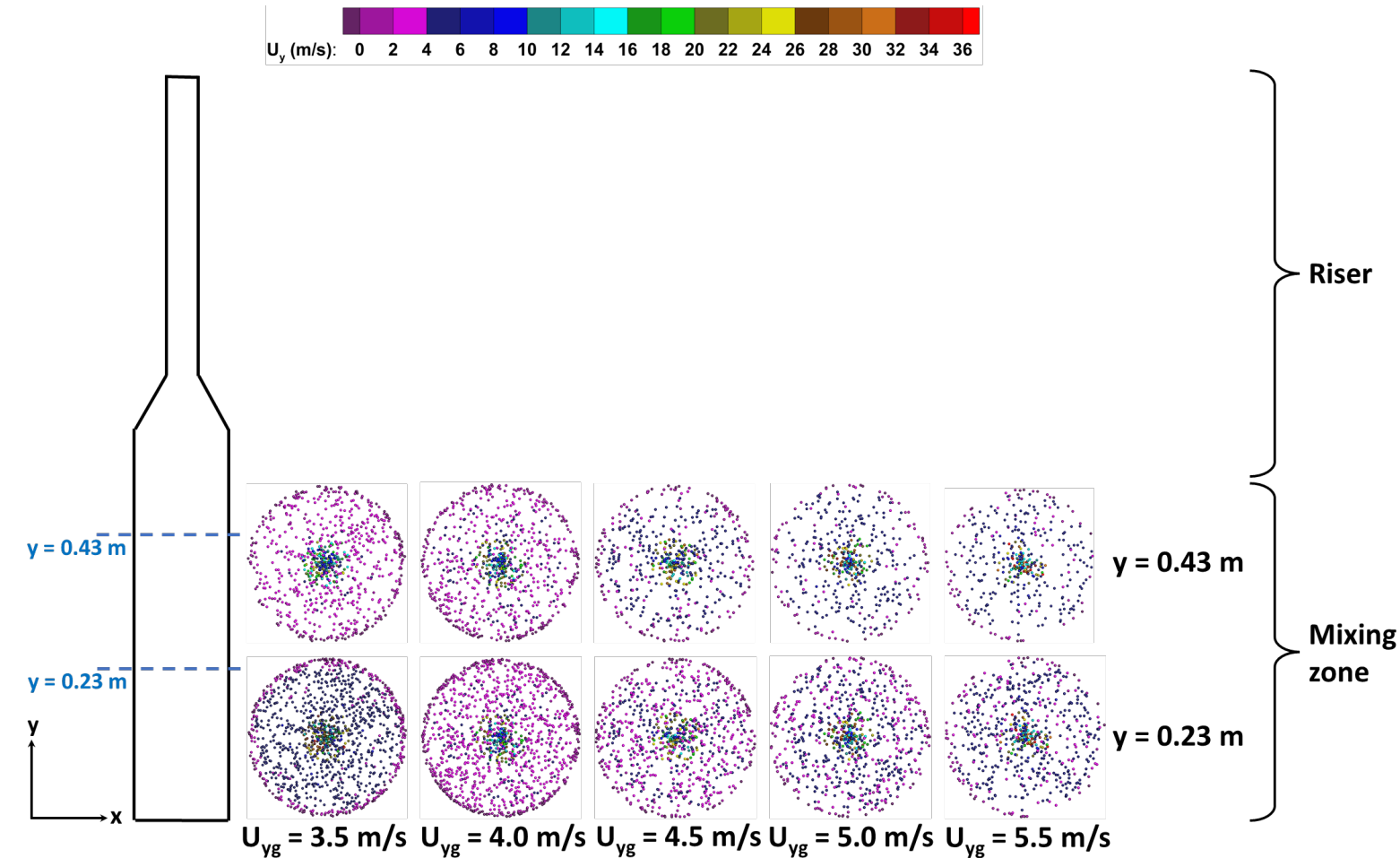


Initial target for the CFB reactor simulation-

- ✓ accurate bed particle expansion
- ✓ interactions of the particles with gas, wall and other particles
- ✓ steady state condition (coking and deactivation analysis)

- Bed particles expand by the combined motion of the fluidizing gas, bed and regenerated particles, gas-solid, P-P and P-W interactions
- Particles begin to leave the computational domain at 0.21 s and a pseudo steady-state is reached at 0.48 s for this run
- At steady state, the particle temperature inside the riser reaches up to 900 K by proper fluidization and mixing

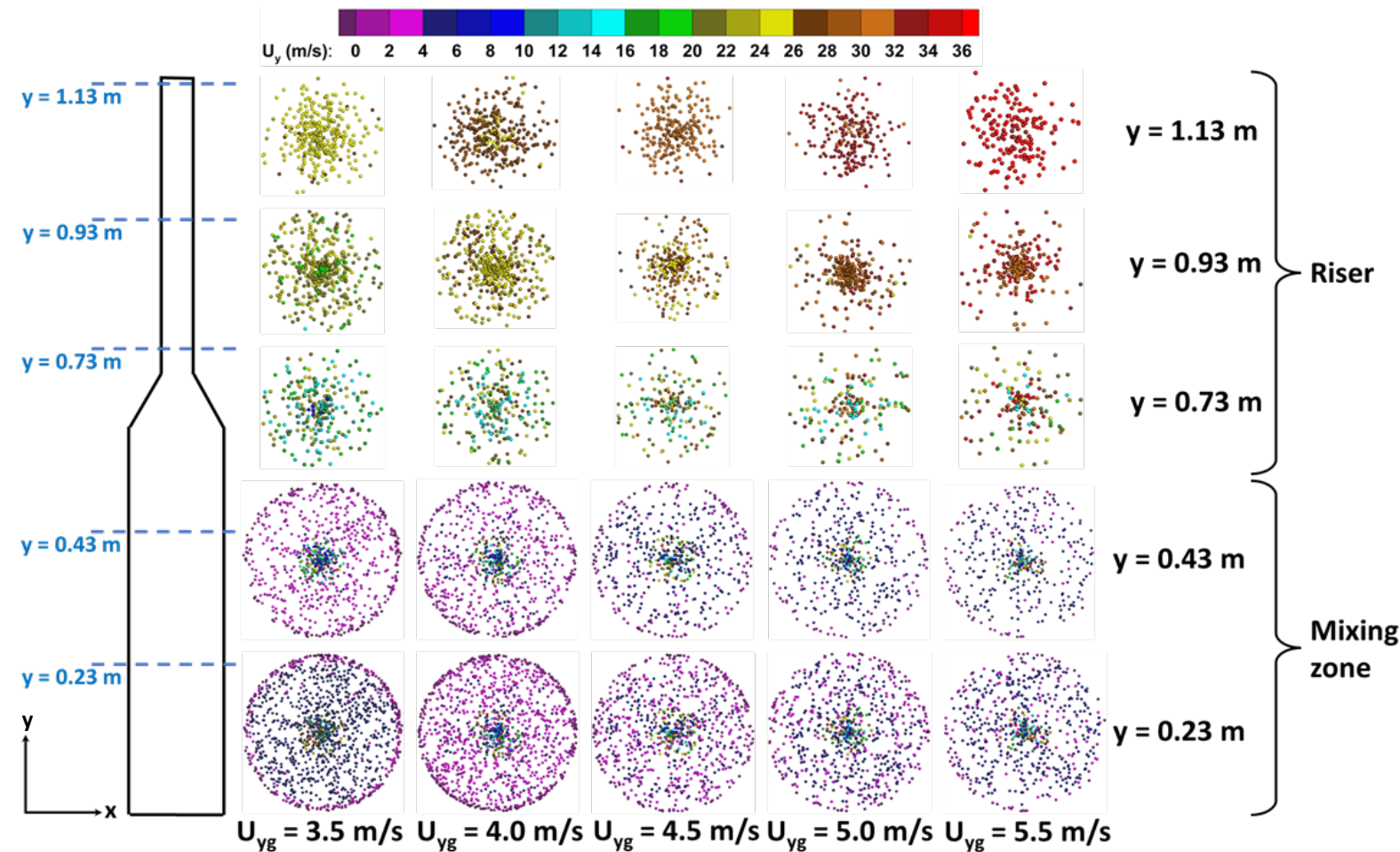
Fluidization and hydrodynamic behavior (simulation without chemical reactions)



- Particles are more crowded near the inlet having most of the bed and regenerated particles interactions
- Reasonably controlled, homogeneous and axisymmetric flow regimes

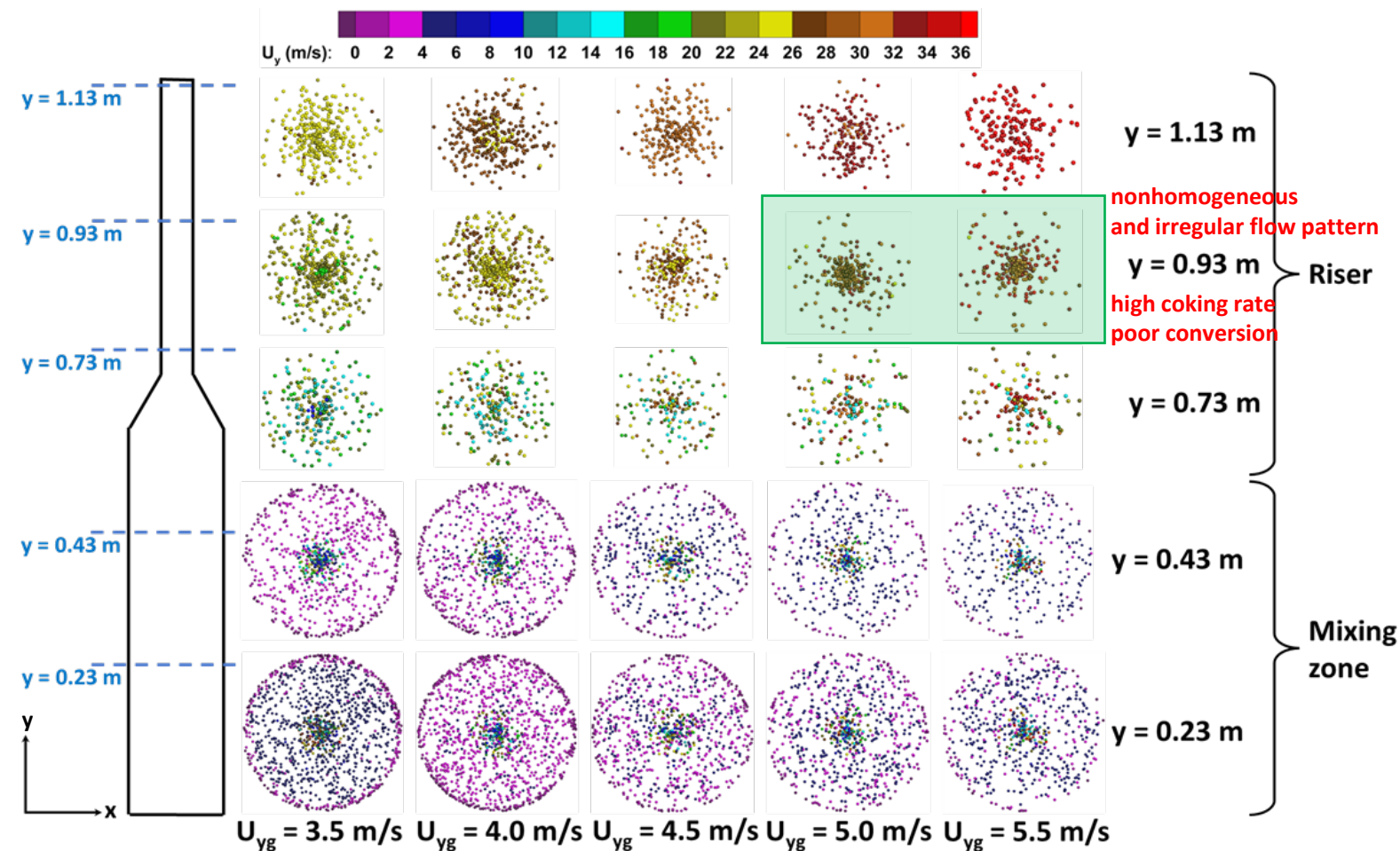
Steady state particle distribution over domain cross section at different axial locations and gas velocities

Fluidization and hydrodynamic behavior (simulation without chemical reactions)



- Particles are more crowded near the inlet having most of the bed and regenerated particles interactions
- Reasonably controlled, homogeneous and axisymmetric flow regimes
- Highly nonhomogeneous and nonuniform flow pattern in the riser section → turbulence, uneven heating rates and residence time
- Indicates the zone with expected high degree of coking, leading to undesirable conditions inside the reactor

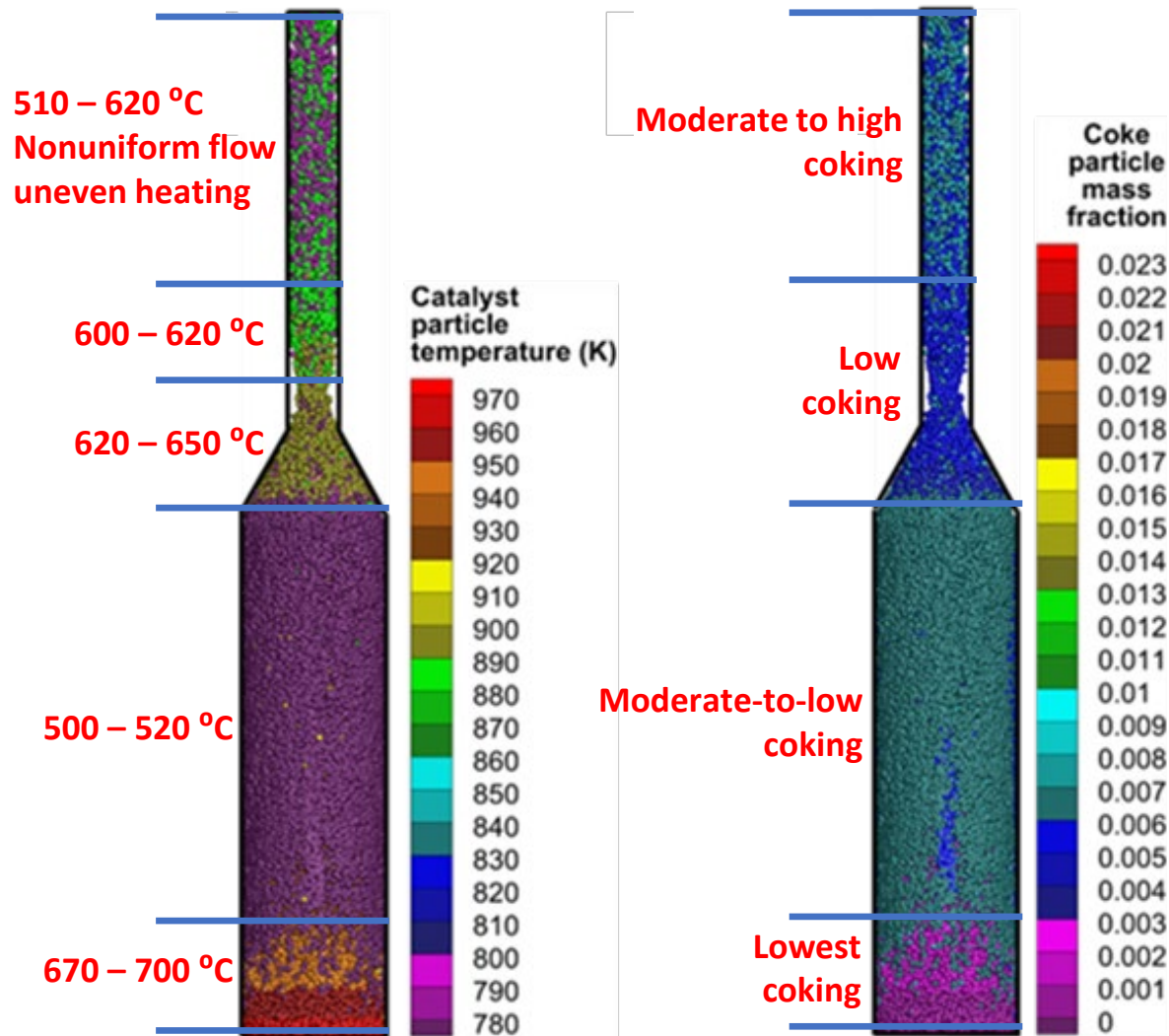
Fluidization and hydrodynamic behavior (simulation without chemical reactions)



Steady state particle distribution over domain cross section at different axial locations and gas velocities

- Particles are more crowded near the inlet having most of the bed and regenerated particles interactions
- Reasonably controlled, homogeneous and axisymmetric flow regimes
- Highly nonhomogeneous and nonuniform flow pattern in the riser section → turbulence, uneven heating rates and residence time
- Indicates the zone with expected high degree of coking, leading to undesirable conditions inside the reactor
- Region specifically needed to investigate further and conditions like to avoid in reactor design

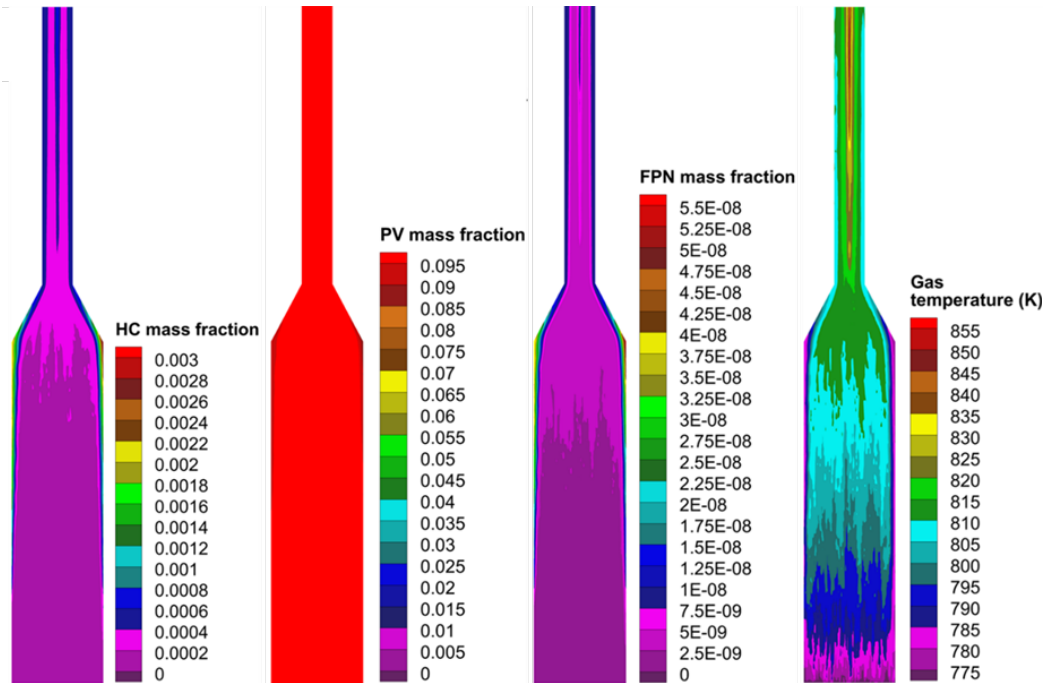
Particle scale coke formation and catalyst deactivation (Reactive simulation with the chemical reaction kinetics)



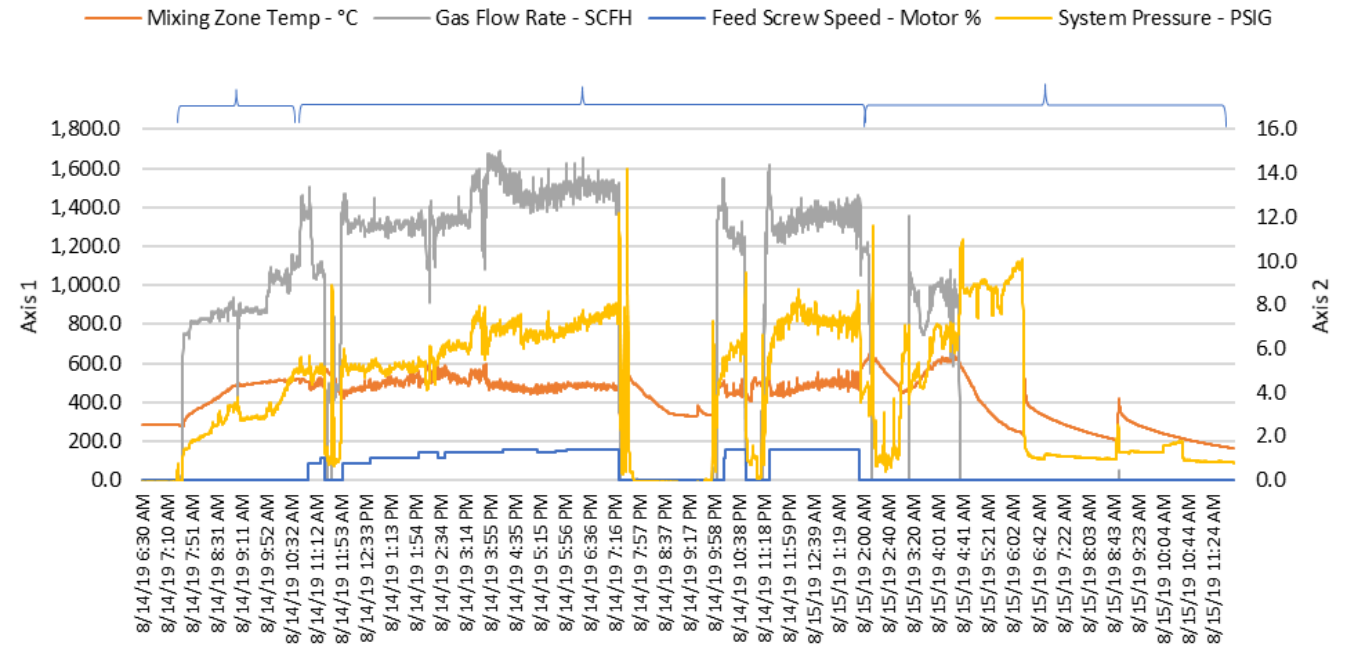
Steady state catalyst particle temperature and coke particle mass fraction distribution in the domain

- Highest temperature near the inlet (fresh regenerated catalysts)
- Lower temperature in the mixing zone due to interaction with the bed particles → moderate to low coking
- Intermediate temperature regime (600 - 650 °C) → low coking
- High coking in the turbulent, nonhomogeneous flow regime of the riser, attributed to the high inlet gas velocity
- Avoid $V_{yg} > 4$ m/s to circumvent uneven heating in the riser turbulent region, leading to lower coking and higher yields

Catalytic upgrading of pyrolysis vapor



Steady state (0.48 s) mass fraction contours of gas phase lumped specie and temperature during the catalytic upgrading



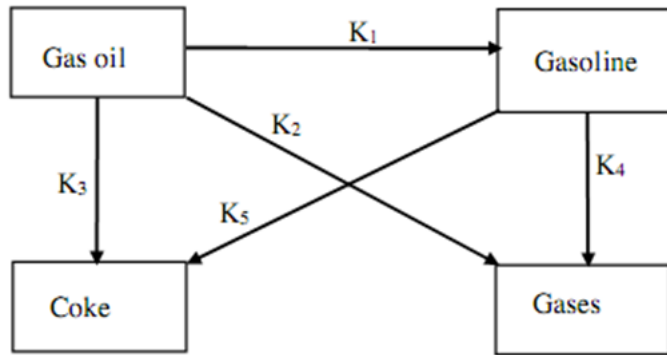
Instrument data for main pyrolysis system variables during RTI pilot scale reactor operations

Challenging to directly compare the experimental findings to simulation results

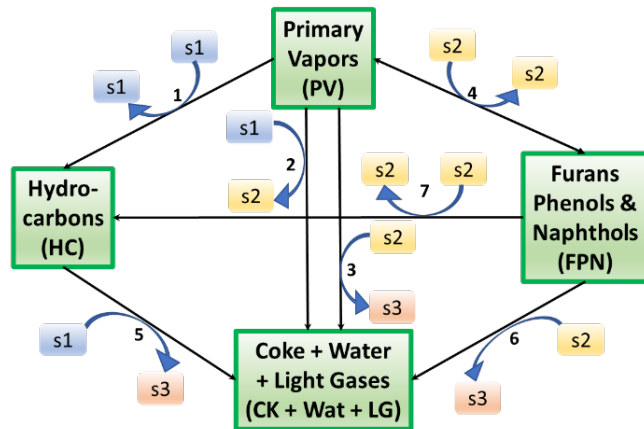
RTI reactor was operated over days with normalized data, whereas pseudo-steady state of the numerical simulation was achieved at 0.48 s

A reactor with designs similar to FCC reactors (originally designed for petroleum cracking) is used for biomass CFP

Comparison of the reaction rate coefficients: 4 lumped kinetic models (directly comparable and easy to implement)



John, Y. M., et al. *Modeling and Simulation of an Industrial Riser in Fluid Catalytic Cracking Process*. in *Computers and Chemical Engineering*. 106 (2017)



Bharadwaj, V., et al. *Extracting Transport Independent Kinetics for Vapor Phase Upgrading of Biomass Pyrolysis Vapors over H-ZSM-5*. in *2018 AIChE Annual Meeting*. 2018. AIChE

Qualitative comparison of the rate factors for FCC and biomass CFP

John et al. four lumped model for FCC		Bharadwaj et al. lumped model for biomass CFP	
Reaction	Frequency factor (s ⁻¹)	Reaction	Rate constant (m ³ /mol.s)
Gas oil → Gasoline (Desired)	1457.50	PV+s1 → HC+s1 (Desired)	2.5728
Gas oil → Coke (Coking)	1.98	PV+s1 → CK+s2 (Coking)	0.4561
Gas oil → C ₁ -C ₄ Gases (Desired)	127.59	PV+s2 → FPN+s2 (Desired)	2.9039
Gasoline → Coke (Coking)	0.00063	FPN+s2 → CK+s3 (Coking)	0.006

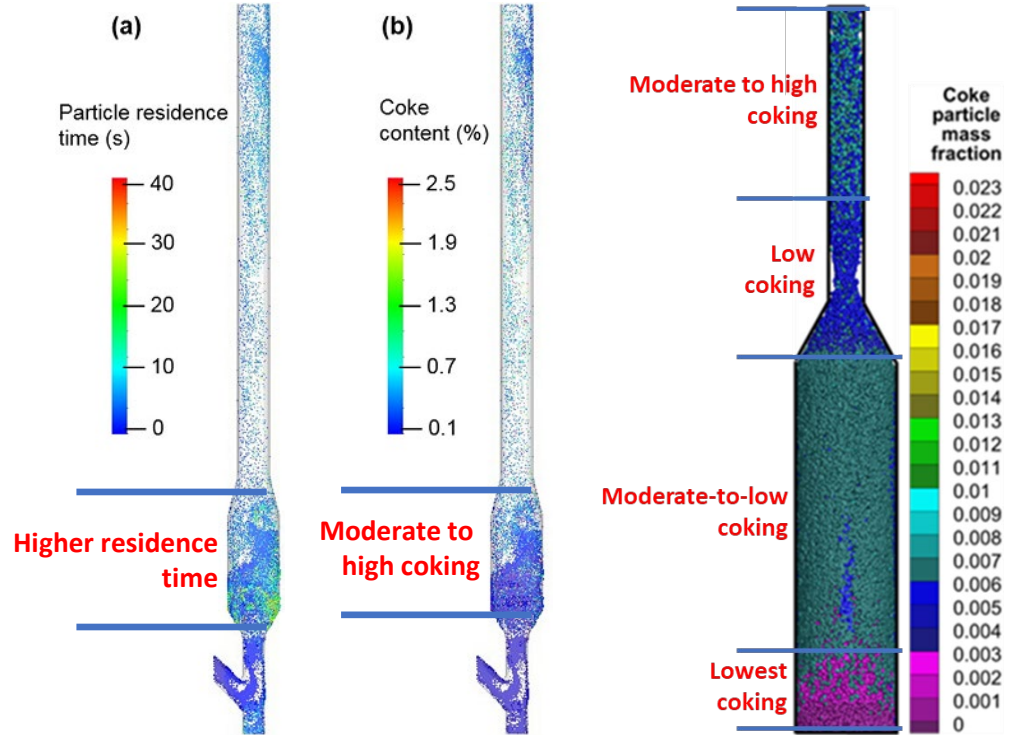
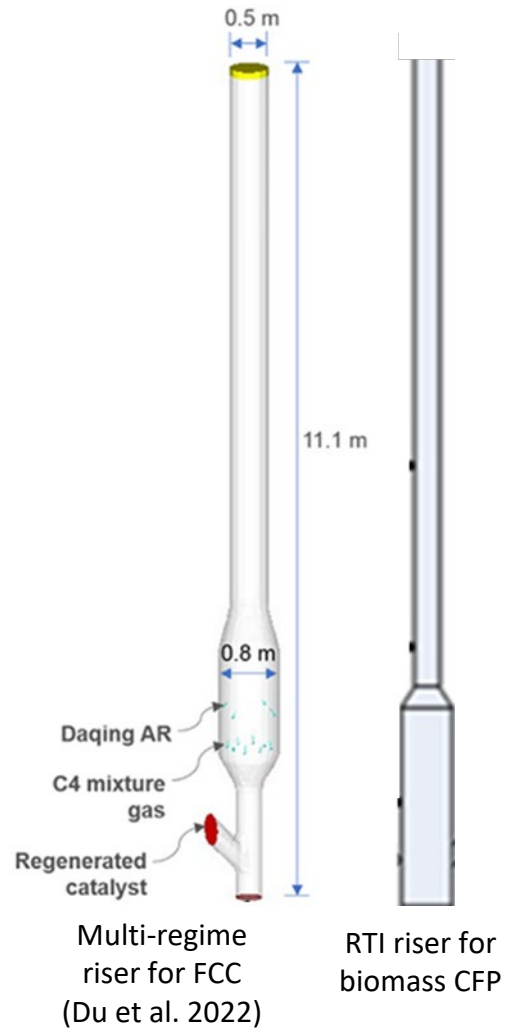
Three orders of magnitude difference

5.6 times different

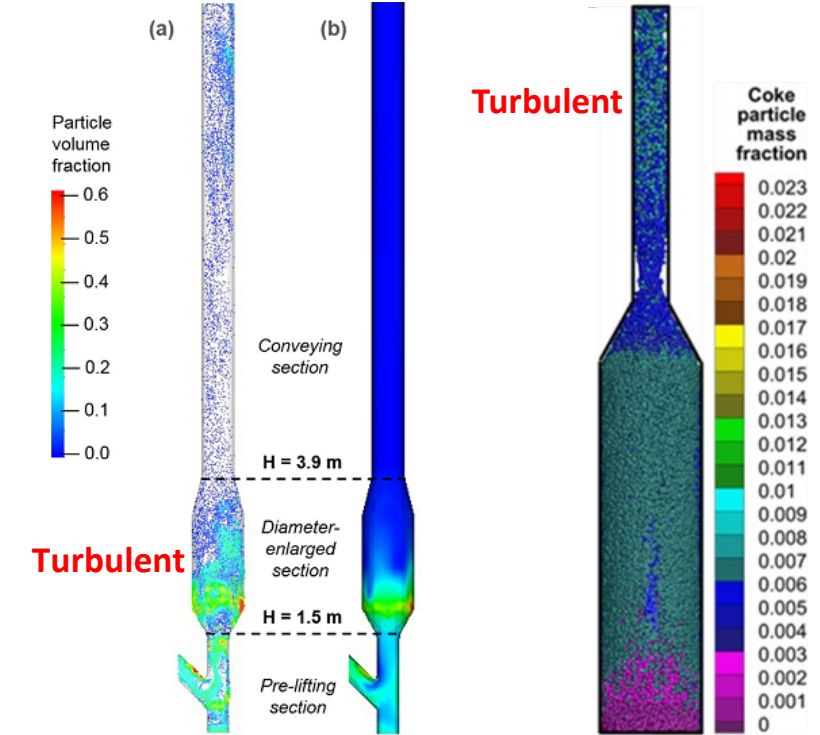
Challenge to design biomass CFP reactors with much controlled residence time, heating rate and flow regimes and more susceptible to coking

A reactor with designs similar to FCC reactors (originally designed for petroleum cracking) is used for biomass CFP

Comparison of the reactor design: multi-regime riser (similar to RTI riser section)



Significantly different coking profiles in FCC and RTI biomass CFP risers

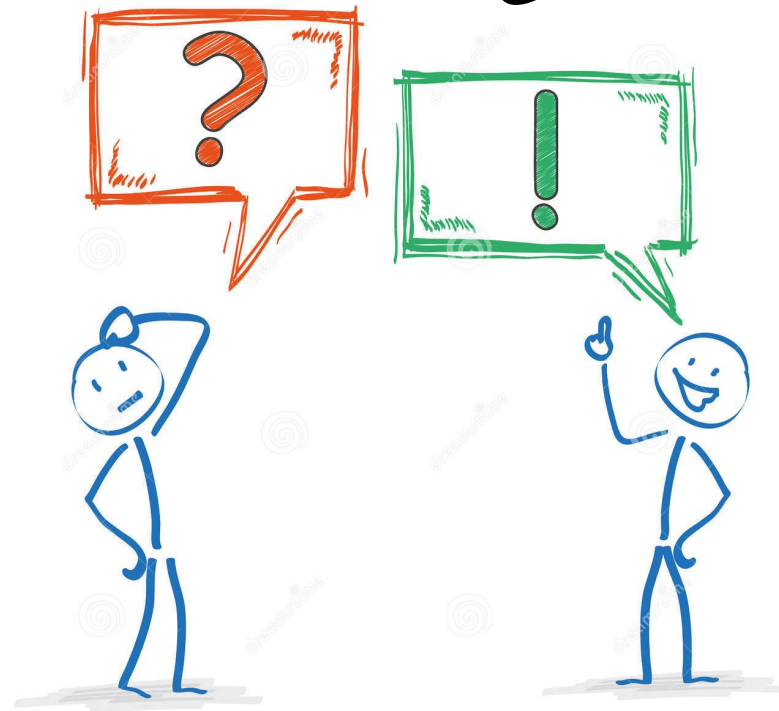


Significantly different flow regimes: different locations of nonlinear and intensely turbulent gas-solid flow

RTI could tune their riser geometry and operating parameters with a multi-regime riser for a better flow phenomena, heating rate and residence time for biomass CFP, leading to an improved yield with reduced coking

- ✓ The CFD-DEM model under MFIX platform works very well in giving detail analysis of the flow inside fluidized bed transport reactor, not possible in experimental configurations
- ✓ The model gives significant insights into areas of the reactor susceptible to coking as well as reactor design
- ✓ A reactor with designs similar to FCC reactors (originally designed for petroleum cracking) is used here for biomass catalytic fast pyrolysis. Since biomass CFP desired Vs coking rates are significantly different than the petroleum cracking desired Vs coking rates (3 orders of magnitude Vs 5.6X), those FCC reactor designs might not translate well to biomass CFP reactor designs. This CFD-DEM analysis could explain that well.
- ✓ A better flow phenomena and residence time could be achieved in RTI biomass CFP reactor by tuned geometry and operating parameters for the riser, leading to higher yield and lower coking

Thank you



Gas phase continuum approach

The flow of gases in dense two-phase system, governed by volume-averaged Navier-Stokes equations:

Gas phase mass conservation

$$\frac{\partial}{\partial t}(\varepsilon_g \rho_g) + \nabla \cdot (\varepsilon_g \rho_g \vec{v}_g) = \sum_{n=1}^{N_g} R_{gn}$$

ε_g = gas phase volume fraction (void fraction)

N_g = number of gas phase chemical species

R_{gn} = rate of formation (or consumption) of gas species n

Gas phase momentum conservation

$$\frac{\partial}{\partial t}(\varepsilon_g \rho_g \vec{v}_g) + \nabla \cdot (\varepsilon_g \rho_g \vec{v}_g \vec{v}_g) = \nabla \cdot \bar{\bar{S}}_g + \varepsilon_g \rho_g \vec{g} - \sum_{m=1}^M \vec{I}_{gm}$$

S_g = gas phase stress tensor

I_{gm} = gas and m^{th} solid momentum exchange

$$\bar{\bar{S}}_g = -P_g \bar{\delta} + \bar{\tau}_g$$

Viscous stress tensor: $\bar{\tau}_g = \mu_g \left(\frac{\partial v_{gi}}{\partial x_j} + \frac{\partial v_{gj}}{\partial x_i} \right) + \mu'_g \left(\frac{\partial v_{gk}}{\partial x_k} \right) \delta_{ij}$ μ'_g = second coefficient of viscosity = $2/3\mu_g$

Gas phase species conservation

$$\frac{\partial}{\partial t}(\varepsilon_g \rho_g X_{gn}) + \nabla \cdot (\varepsilon_g \rho_g \vec{v}_g X_{gn}) = \nabla \cdot \left(\varepsilon_g \rho_g D_{gn} \frac{\partial X_{gn}}{\partial x_i} \right) + \sum_{n=1}^{N_g} R_{gn}$$

X_{gn} = mass fraction of n^{th} gas species

D_{gn} = diffusivity of n^{th} gas species

Gas phase energy conservation

$$\varepsilon_g \rho_g C_{pg} \left(\frac{\partial T_g}{\partial t} + \vec{v}_g \cdot \nabla T_g \right) = -\nabla \cdot \left(-\varepsilon_g \kappa_g \frac{\partial T_g}{\partial x_i} \right) + q_{gs} - \Delta H_{rg}$$

C_{pg} = gas phase specific heat

κ_g = gas phase thermal conductivity

q_{gs} = gas-solid interphase energy transfer

ΔH_{rg} = heat of reaction

Gas phase EOS for density

$$\rho_g = P_g M_g / RT_g$$

Coupling the gas-solid interaction forces

The gas and m^{th} -solid phase momentum exchange:

$$I_{gm} = \frac{1}{V_c} \sum_{i=1}^{N_p} F_{tot}$$

F_{tot} = summation of the drag and pressure gradient force of particles in the computational cell of volume V_c

$$F_{tot} = \frac{CV_i}{1-\varepsilon_g} (\vec{u}_g^i - \vec{v}_p) + (-\nabla P_g^i V_i)$$

V_i = volume of particle i

u_g^i = gas velocity interpolated at particle i

ΔP_g^i = pressure gradient interpolated at particle i

Interphase momentum exchange term C correlation (Not resolved by numerical discretization- $\Delta x_{\text{gas phase}} \gg D_p$)

Gidaspow model:

$$C = \frac{150(1-\varepsilon_g)^2 \mu_g}{\varepsilon_g d_p^2} + 1.75 \frac{(1-\varepsilon_g) \rho_g |\vec{u}_g - \vec{v}_p|}{d_p}, \varepsilon_g \leq 0.8$$

$$= \frac{3}{4} \frac{\varepsilon_g (1-\varepsilon_g) \rho_g |\vec{u}_g - \vec{v}_p|}{d_p} C_D \varepsilon_g^{-2.65}, \varepsilon_g > 0.8$$

$$C_D = \frac{24}{\text{Re}_p} (1 + 0.15 \text{Re}_p^{0.687}), \text{Re}_p < 1000$$

$$= 0.44, \text{Re}_p \geq 1000$$

$$\text{Re}_p = \frac{\varepsilon_g \rho_g |\vec{u}_g - \vec{v}_p| d_p}{\mu_g}$$

Interphase heat transfer methods

Solid phase (particle) internal energy conservation

$$m^{(i)} C_{PP}^{(i)} \frac{dT_p^{(i)}}{dt} = \underbrace{\dot{Q}_{PP}^{(i)} + \dot{Q}_{Pfp}^{(i)} + \dot{Q}_{Pg}^{(i)} + \dot{Q}_{rad}^{(i)}}_{\text{Interphase heat transfer}} - \Delta H_{rs}$$

$m^{(i)}$ = mass of particle i
 $C_{PP}^{(i)}$ = specific heat of particle i
 $T_p^{(i)}$ = temperature of particle i
 ΔH_{rs} = heat of reaction supplied to the solid phase + enthalpy transfer due to mass transfer

Solids phase: all particles with same density ρ_{sm} and diameter D_m

Interphase heat transfer for particle i : $q_{gs}^i = \underbrace{q_{pp}^i}_{\text{Contact conduction}} + \underbrace{q_{pfp}^i}_{\text{Particle-fluid-particle conduction}} + \underbrace{q_{pg}^i}_{\text{Gas-particle convection}} + \underbrace{q_{rad}^i}_{\text{Particle-environment radiation}}$

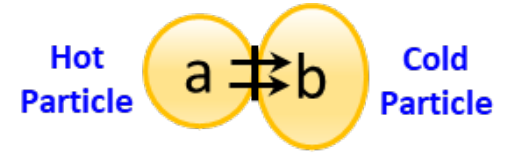
Negligible P-P, P-W and P-G radiative heat transfer

Energy transfer from a hot to a cold particle through their shared area of contact in the dense particulate system (Batchelor and O'Brien model):

Contact conduction

$$\dot{Q}_{pp}^{(ij)} = \frac{4\kappa_p^i \kappa_p^j}{\kappa_p^i + \kappa_p^j} (T_p^j - T_p^i) \sqrt{(R_p^j)^2 - \left(\frac{(R_p^j)^2 - (R_p^i)^2 + (l^{ij})^2}{2l^{ij}}\right)^2}$$

κ_p = Effective thermal conductivity
 T_p = Temperature
 R_p = Contact radius of particles i and j
 $l^{(i,j)}$ = distance between the particle centers

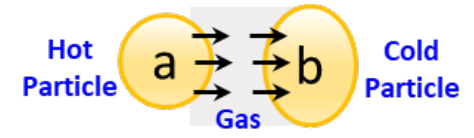


Energy transfer by conducting heat through the stagnant gas between two particles of proximity (modified Rong and Horio correlation):

Particle-gas-particle (pgp) conduction

$$\dot{q}_{pfp}^{(i,j)} = \kappa_g (T_p^{(j)} - T_p^{(i)}) \int_{R_c}^{R_f^{(i,j)}} \frac{2\pi r}{l^{(i,j)} - ((R_p^{(i)^2} - r^2)^{1/2} - (R_p^{(j)^2} - r^2)^{1/2})} dr$$

$$R_c = \begin{cases} 0 & \text{for } l^{(i,j)} > 2R_p \\ \tilde{R}_c^{(i,j)} & \text{for } l^{(i,j)} \leq 2R_p \end{cases} \quad \tilde{R}_c^{(i,j)} = \sqrt{R_p^{(k)^2} - \left(\frac{R_p^{(k)^2} - R_p^{(l)^2} + l^{(i,j)^2}}{2l^{(i,j)}}\right)^2}$$



$$R_f^{(i,j)} = \sqrt{(R_p^{(k)} + d^{(k)})^2 - \left(\frac{(R_p^{(k)} + d^{(k)})^2 - R_p^{(l)^2} + l^{(i,j)^2}}{2l^{(i,j)}}\right)^2}$$

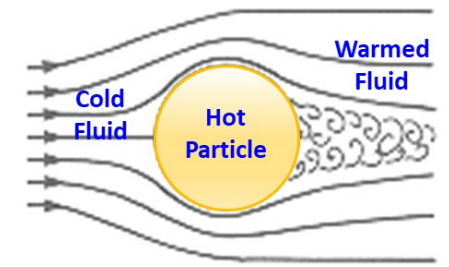
$R_p^{(k)}, R_p^{(l)}$ = larger and smaller particle radius
 $d^{(k)}$ = gas layer thickness of particle $k = R_p^{(k)}/5$

The convective energy transfer between a particle and its surrounding gas (Ranz and Marshall correlation):

Gas-particle convection

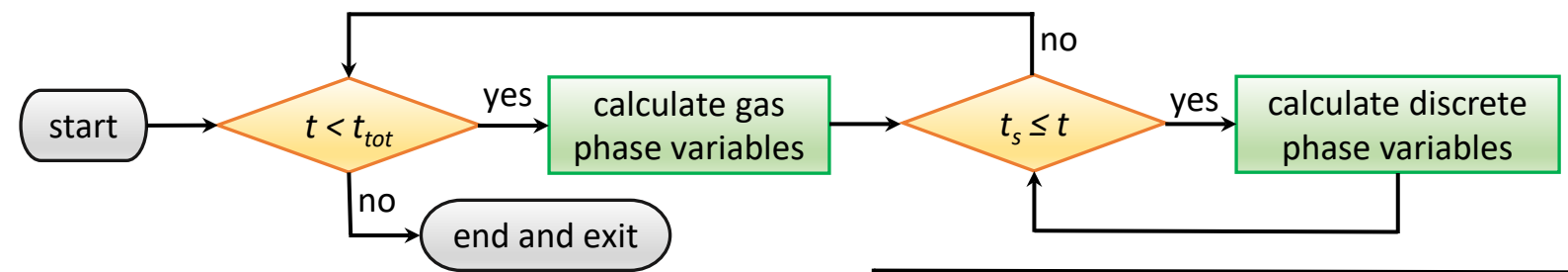
$$\dot{q}_{pg} = \gamma_{cp} A_s (T_g - T_p)$$

$$\gamma_{cp} = \frac{Nu \cdot \kappa_g}{2R_p} \quad Nu = 2.0 + 0.6 Re^{1/2} Pr^{1/3} \quad Re = \frac{\rho_g \epsilon_g |v_g - v_p| 2R_p}{\mu_g} \quad Pr = \frac{C_{pg} \cdot \mu_g}{\kappa_g}$$



Fluid step forward – Particle catch-up process

Determines when information is exchanged between gas and particles to computationally connect gas and discrete solid phases



- Gas phase takes a step forward in time to solve the variables
- Several smaller time steps are taken by the solid phase to allow the particles to catch up
- Fluid properties are constant at the last converged value while the solids are calculated and vice versa

t = fluid most recent solution time
 t_{tot} = total specified solution time
 t_s = solid most recent solution time

